Volitional muscle activation intensifies neuronal processing of proprioceptive afference in the primary sensorimotor cortex: an EEG study

RESEARCH ARTICLE

RUNNING HEAD: Motor output intensifies cortical proprioceptive processing

Volitional muscle activation intensifies neuronal processing of proprioceptive afference in the primary sensorimotor cortex: an EEG study

Alessandra Giangrande[1-2], Giacinto Luigi Cerone[2], Alberto Botter[2], and Harri Piitulainen[1]

[1]Faculty of Sport and Health Sciences, University of Jyväskylä, Jyväskylä, Finland

[2]Laboratory of Neuromuscular System and Rehabilitation Engineering, DET, Politecnico di Torino, Turin, Italy

Correspondence: Alessandra Giangrande, e-mail: alessandra.giangrande@polito.it / alessandra.x.giangrande@jyu.fi.

ABSTRACT

Proprioception refers to the ability to perceive the position and movement of body segments in space. The cortical aspects of the proprioceptive afference from the body can be investigated using corticokinematic coherence (CKC). CKC accurately quantifies the degree of coupling between cortical activity and limb kinematics, especially if precise proprioceptive stimulation of evoked movements are used. However, there is no evidence on how volitional muscle activation during the proprioceptive stimulation affects CKC strength. Twenty-five healthy volunteers (28.8 ± 7 yr, 11 females) participated the experiment that included electroencephalographic (EEG), electromyographic (EMG) and kinematic recordings. 2-Hz ankle-joint rotations were elicited through a movement actuator in two conditions: *passive* condition with relaxed ankle and *active* condition with constant 5-Nm plantar flexion exerted during the stimulation. In total, 6-min of data were recorded per condition. CKC strength was defined as the maximum coherence value among all the EEG channels at the 2-Hz-movement frequency for each condition separately. Both conditions resulted in significant CKC peaking at the Cz electrode over the foot area of the primary sensorimotor (SM1) cortex. Stronger CKC was found for the *active* (0.13 ± 0.14) than passive (0.03 ± 0.04) condition ($P < 0.01$). The results indicated that volitional activation of the muscles intensifies the neuronal proprioceptive processing in the SM1 cortex. This finding could be explained both by peripheral sensitization of the ankle joint proprioceptors and central modulation of the neuronal proprioceptive processing in the spinal and cortical levels.

NEW & NOTEWORTHY

The current study is the first to investigate the effect of volitional muscle activation on CKC-based assessment of cortical proprioception of the ankle joint. Results show that the motor efference intensifies the neuronal processing of proprioceptive afference of the ankle joint. This is a significant finding as it may extend the use of CKC method during active tasks to further evaluate the motor efference-proprioceptive afference relationship, and the related adaptations to exercise, rehabilitation and disease.

Keywords: Corticokinematic coherence, Electroencephalography, Proprioception, Somatosensory

INTRODUCTION

Motor control in humans relies on the combination of a multitude of senses regulated by sensory systems such as the visual, vestibular, and somatosensory system which are responsible of informing the central nervous system (CNS) about the environment and the body itself (1, 2). Proprioception is part of the somatosensory system and it measures the internal state of the musculoskeletal system being responsible for providing information to the CNS about the position, movement and dynamics of the musculoskeletal system (3). Proprioception encompasses various senses related to changes in the internal state of the locomotor system and it is restricted to the ones that can be consciously perceived. These include, e.g., the sense of movement, the sense of balance, the sense of joint position, and the sense of force and heaviness (i.e. the sense of effort) (4). These sensations arise from peripheral signals generated by various types of receptors (i.e. proprioceptors) located in the muscles, joints, ligaments and soft tissues around the joints (5). Proprioceptors are mechanoreceptors which activity is modulated by bodily movements changing the muscle length (muscle spindles) or muscle tension (Golgi tendon organs). Proprioceptive signals can be further integrated with closely related information from cutaneous tactile mechanoreceptors sensitive to stretch of the skin during joint rotation (e.g., Pacinian corpuscles), thus providing specific “fingerprints” of certain movements to the CNS (4, 6).

Afferent proprioceptive pathways to the brain travel primarily along the afferent dorsal column-medial lemniscus first to the thalamus where the signals are further relayed to the cortex (7). Here the brain integrates the proprioceptive afference with inputs from other senses, such as vison or touch, carrying information from the external environment (4). Specifically, the primary sensorimotor cortex (SM1) is the site where the basic sensorimotor integration (i.e. the integration of sensory information from multiple sources aimed at producing task-specific motor output) occurs.

Proprioception has a crucial role in motor control as it provides essential rich regulatory feedback about the internal state of the locomotor system to the CNS (1). First, it is fundamental for joint stabilization in postural control and balance (8). Second, it is crucial to motor planning (feedforward strategy) rapidly signalling the brain allowing for anticipation, preparation, and response planning (9). Third, recent evidence supported the view that the proprioceptive afference is one of the key sensory modalities supporting motor learning (10, 11). Through proprioception it is also possible for the CNS to fine tune the ongoing motor command or action and thus produce smooth, appropriate motor actions, which is especially important for targeted movements of the limbs (feedback strategy) (12).

The relevance of proprioception in all human actions has encouraged researchers over decades to investigate the proprioceptive sense also at the cortical level (7, 8, 13–15). The majority of studies has utilized electroencephalography (EEG) or magnetoencephalography (MEG) in combination with stimulation of the proprioceptors using evoked joint rotations while the participant is at rest (14). The temporal and amplitude features of the neuronal cortical processing of the proprioceptive afference can then be examined by means of the averaged cortical activity time-locked with movements (i.e. evoked responses) (16, 17). In addition to the evoked responses, a recent approach proposed a robust quantification of the degree of cortical proprioceptive processing using corticokinematic coherence (CKC) (18, 19). Jerbi et al. (2007)

first demonstrated using MEG that hand movement velocity and SM1 cortex activity are correlated at the movement frequency (20). The CKC term was later introduced by Bourguignon et al., (2011) (21) and they proposed CKC as a tool for functional motor mapping of the hand region (i.e. locate the cortical origin for the coupling) using MEG and volitional continuous rhythmic movements. Later, it was demonstrated that CKC primarily reflects cortical proprioceptive processing by comparing CKC between active volitional and passive evoked movements. The contribution of corticospinal motor efference to CKC was negligible with respect to the somatosensory afference to the SM1 cortex (22–24). In addition, it was suggested that the strength of CKC can be used to quantify the degree of cortical proprioceptive processing. CKC strength ranges from 0 (no coupling) to 1 (perfect coupling) peaking at the frequency of the movement and its harmonics, following the somatotopy (25). CKC can be quantified using any peripheral signal (e.g. acceleration, force, electromyography, etc.) picking the rhythmicity of the movement (26).

To date, several CKC studies have examined proprioception using movement actuators in passive (resting) conditions (27, 28). CKC strength has been shown to be influenced by factors such as the directed attention to the stimulus (29), the regularity of the stimulation (30), the movement range (18), the number of joints stimulated simultaneously (31), aging (32) or neurological disabilities (e.g. cerebral palsy) (33). Furthermore, reproducibility of CKC is high across experimental sessions both for MEG- and EEG- based measurements (28, 34) although MEG provides somewhat stronger CKC, because of the higher signal-to-noise-ratio (35).

Despite the broad spectrum of studies attempting to understand the mechanisms behind CKC, there is no evidence how volitional muscle activation during the proprioceptive stimulation affects CKC strength. The motor efference is expected to alter the somatosensory afference to the brain via input to the muscles but also more generally to the spinal neuronal circuits (6). In addition, even light volitional muscle contraction can alter the muscle-tendon unit mechanics with respect to the relaxed passive condition. During volitional muscle contraction, the intrafusal fibers of the muscle spindles are also activated by the gamma motor neurons and thus the stretch-sensitivity of the spindle afferents are enhanced (6, 36, 37). Finally, the volitional muscle contraction also modifies the functional state of the SM1 cortex with respect to the passive condition that may likely alter the cortical processing of the proprioceptive afference.

With the present study we aimed to examine the effect of volitional muscle activation on neuronal processing of proprioceptive afference in the human neocortex when quantified using CKC and EEG. We hypothesised that volitional plantarflexion during proprioceptive stimulation (i.e. continuous actuated ankle-joint rotations at 2 Hz) of the ankle joint would strengthen CKC when compared to a condition in which the ankle remains passive. The mechanisms are expected to be due to 1) motor efference-related sensitization of the peripheral proprioceptors through mechanical and neuronal factors and to 2) alterations in the neuronal proprioceptive processing in the spinal and cortical levels. Assessing the sensitivity of CKC to volitional muscle activation is relevant to better understand methodological aspects of CKC and to provide new insight into the neurophysiological processes underlying the complex interactions between the periphery and the brain.

MATERIALS AND METHODS

Participants

A total of 25 young, healthy adults (age 28.8 ± 7 mean ± SD, 11 females) were recruited for the study. The majority of the participants was right-footed (only 2 out of 25 were left-footed) based on Waterloo footedness inventory score that was on average 42 ± 32 on a scale from –100 to

100. All participants reported their right hand as the writing hand. Participants were provided with a complete description of the study procedure after which they were asked to sign a written informed consent. The study was conducted in accordance with the Declaration of Helsinki and its approval was obtained by the Ethics Committee of the University of Jyväskylä before starting the measurements (approval number: 369/13.00.04.00/2020).

Experimental design and recordings

The measurements were conducted at the Faculty of Sports and Health Sciences of the University of Jyväskylä, Jyväskylä, Finland. Proprioceptive-perception ability of the ankle joint was tested first (38, 39). Then, a short (i.e. 30 s) resting state recording was performed and further taken as a baseline. Finally, CKC during ankle joint rotations was quantified for two conditions of the plantar flexor muscles: (1) active condition with steady 5-Nm plantar flexion and (2) passive condition with no plantar flexion torque exerted. The mechanical rotations (i.e. perturbations) were identical between the conditions. The two conditions were measured in four 3-min trials (two trials per condition) with a short brake in between in random order, to avoid effects from any systematic time dependent effects during the recording session.

Experimental Setup

Figure 1 shows the experimental setup adopted for the study. Participants were sitting in a chair with the forearms laying on the armrests and the left foot relaxed on a separate footstool. The right foot was placed on the rotating platform of a motorized ankle-movement actuator. The anatomical ankle-joint rotation axis was identified according to Isman et al., (1969) (40), and it was aligned with the axis of the rotating platform. Ankle and knee joint angles were set to 90°.
During the experiment, EEG and electromyographic (EMG) signals were recorded synchronously with foot angular displacement and torque. Participants were instructed to completely relax their left leg throughout the recordings. Additionally, they wore shielded earplugs (ER-3C, 50 Ohm, Etymotic Research) playing 60 dB Brownian noise to ascertain masking of any, although minute, auditory noise caused by the ankle-movement actuator. No vibrations were generated either at rest or during the stimulations. Visual contact to the stimulated foot was blocked by using a brown cardboard panel while a screen was placed 1.5 m in front of the participants.

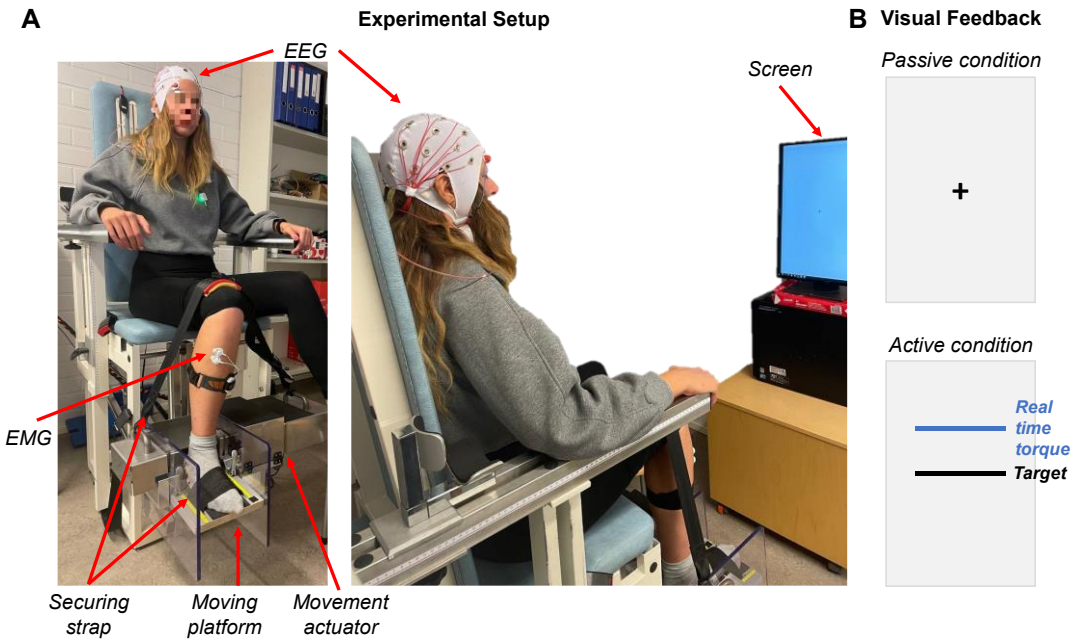

Figure 1 – Experimental Setup. A) Participant's right foot was placed on the rotating platform with knee and ankle joints at 90°. 30 EEG, 2 EOG channels and EMG, electromyographic signals from right soleus and tibialis anterior were recorded. B) Visual feedback varied between the conditions. A fixation cross was shown during the passive condition, and the real-time torque with 5 Nm target level were shown during the active condition.

Movement actuator

Proprioceptive stimuli (i.e. ankle rotations) were produced using a custom-made silent ankle-movement actuator. It was composed of a rotating platform driven by a servomotor controlling the rotations according to the desired angular velocity (full operational range: 0–200 °/s) managed by a control unit. The platform was equipped with torque and angular displacement sensors, that were interfaced to a control unit generating analogue output signals in the range of 0–5 V. The stimulation patterns were controlled using a custom-made Graphical User Interface (Matlab R2022b, MathWorks Inc, Natick, MA, USA) that was configured to handle real-time visualization and storage of the data. A data acquisition unit (USB-6216 AD-board, National Instrument Austin, Texas, United States) was, indeed, configured as an I/O board communicating with the proprioceptive stimulator and it was set through Matlab software to deliver the stimulation patterns and to acquire analog torque and joint angle signals (sampling frequency of 1 kHz).

EEG recordings

A wireless light weight EEG amplifier (41–43) was used to record EEG signals with a 30 Ag/AgCl electrodes cap (EasyCap GmbH, Gliching, Germany) following the international 10-20 system. To ensure a good skin-electrode contact, each electrode site has been gently scrubbed through a cotton swab with an abrasive paste (NuPrep, Weaver and Company, Aurora, USA) and then filled with a conductive gel (NeurGel, SPES MEDICA, Genova, Italy). Additionally, electro-oculogram (EOG) signals were acquired through two surface electrodes (30 mm × 22 mm Ambu s.r.l., Denmark) placed in the up-left and down-right corners of the eye region. EEG and EOG signals were acquired in a monopolar derivation, using the FCz electrode of the cap as the reference with a sampling frequency of 2048 Hz, and a bandwidth of 0.1–500 Hz. EEG signals were collected synchronously with EMG and they were offline synchronized with kinematic signals according to a common external trigger by using the synchronization unit introduced in (41).

EMG recordings

EMG were recorded from the tibialis anterior muscle and right medial part of the soleus muscle using a pair of Ag/AgCl electrodes (Ø 24 mm Kendall, Covidien, Dublin, Ireland) placed on each muscle according to the SENIAM recommendations (44) after a gentle skin abrasion of the interested area by using an abrasive paste (Nuprep, Weaver and Company, Aurora, USA) (45). EMG was acquired in a bipolar derivation through a wireless amplifier (DuePro, OT Bioelettronica, Turin, Italy) with a sampling frequency of 2048 Hz in the 10–500 Hz frequency band.

Proprioceptive-perception ability

To test the correlation between the neurophysiological and the behavioral measurements, the perceptual proprioceptive threshold was computed for each participant. Perceptual threshold of the evoked ankle joint rotation was defined for the right leg using the proprioceptive stimulator and an adaptive-test algorithm (38). The right ankle was passively dorsiflexed at a varying angular velocity from 0.3 to 1.5°/s (inter stimulus interval: 4 ± 0.25 s). Participants were instructed to fixate a black cross on a grey background on the screen in front of them, and to press a response button with their right thumb as soon as they perceived the movement of the platform. The analogue output of the response button was sampled at 1 kHz through the I/O board and it was used as a marker of the rotation perception. The detection or missing of a stimulus was utilized to adapt the angular velocity (i.e. decrease or increase of 0.1°/s) of the subsequent stimulus allowing for the identification of the individual proprioceptive threshold. The proprioceptive-perception threshold was defined as the lowest angular velocity with >50% correctly perceived stimuli and it was automatically updated throughout the test after each stimulus. The experimenter manually stopped the test if two criteria were met: (1) a minimum of 5 stimuli at the threshold velocity were provided to the participant and (2) at least a total of 25 rotations were delivered during the test.

Corticokinematic coherence

To compare the degree of cortical proprioceptive processing during the *active* and *passive* conditions, CKC was computed. The right ankle joint was stimulated at 2-Hz with a continuous 4° ankle rotation in dorsi and plantarflexion direction (8° total range of motion) at 25°/s angular velocity 3 min per condition and trial (in total 6 min of data per condition). A screen was placed 1.5 m in front of the participants to provide a visual feedback during the tested conditions. During the *passive* condition, participants were instructed to relax their lower limbs and to fixate at a black cross on the screen in front of them. During the *active* condition, participants were instructed to apply a constant plantarflexion torque of 5 Nm (± 2.5 Nm) about the axis of the rotating platform, and they were provided with a visual real-time feedback displaying the applied torque and the desired target (Figure 1 B). The experimental design was planned to prevent visual contamination of CKC at the movement frequency. To this end, the torque feedback displayed on screen to the participants was computed by averaging the torque signal over a 600 ms moving epoch with 300 ms overlap. This approach prevented continuous oscillation of the displayed torque signal at the 2-Hz proprioceptive stimulation frequency that could have led to strong CKC in the occipital visual cortices and consequent bias in our SM1 cortex CKC strength. Finally, to prevent any vertical raise of the heel from the rotating platform, the sole of the right foot was secured to the platform using a strap around the knee and an elastic Velcro around the midfoot. EMG signals were real-time inspected by the experimenter to ascertain that the participant was relaxed during the *passive* condition. The experimental setup was the same in the two experimental conditions. The order of the *active* and *passive* conditions was randomized, with the starting condition balanced across participants. Each recording always started with 30-s rest period followed by 3 min stimulation.

Signal analysis

Signal processing was entirely performed offline in Matlab R2022b (Mathwork Inc, Natick, MA, USA). Angular displacement and torque signals were resampled at 2048 Hz to match with EEG and EMG signals. An offline synchronization was performed by aligning all the recorded signals according to the rising edge of a common external trigger sent at the beginning of each trial.

EEG and EMG signal preprocessing

FieldTrip Matlab toolbox was used for the EEG analysis (46). EEG data were first visually inspected to identify and mark the noisy channels. Then, EEG signals were bandpass filtered through a 4^{th} order Butterworth filter at 0.1–95 Hz, and independent component analysis was used to extract 30 EEG independent components to identify those related to artifacts (e.g. due to eye movements or neck/temporalis muscular activity). Eye blinks or eye movements were identified based on the highest correlation with the EOG pattern and then they were removed. Only after the independent component analysis, noisy channels were interpolated by replacing them with the average of all the neighboring channels. Finally, a common average reference was applied to all EEG channels (47).

EMG signals were offline bandpass filtered at 20–400 Hz with 4^{th} order Butterworth filter.

Corticokinematic coherence analysis

The formulation of Halliday et al., (1995) (48) was used to compute the coherence between EEG and the angular-displacement signal (i.e., the foot kinematics). EEG signals were split into 2-s epochs with 1.6 s overlap, yielding a frequency resolution of 0.5 Hz (49). EEG epochs exceeding 200 mV were considered to be corrupted by artifacts and were rejected. Coherence computation yielded cross-, power- and coherence spectra between the foot kinematics and each EEG signal separately. The magnitude squared coherence was chosen as coupling measure as done in earlier CKC studies (19, 21, 28). CKC strength was defined as the coherence value at the 2-Hz movement frequency in the peak EEG channel among all the 30 EEG channels for each participant and condition. Then, averaged CKC value of the two trials for *active* or *passive* condition was used as final CKC strength estimate for each participant. For visualization purposes, CKC spectra from the two trials of the same condition were also averaged separately for each participant and topographic representations of CKC were further visualized at the group level.

Statistical analysis

All results are given as mean ± SD. Statistical tests were performed in Matlab R2022b on the averaged data across the trials for both *active* and *passive* conditions (Mathwork Inc, Natick, MA, USA). We tested the normal distribution of the data through a Shapiro-Wilk test for each condition. All the variables were non-normally distributed ($P < 0.05$), thus we used nonparametric statistical tests for the statistical analysis.

EMG activity during CKC testing

EMG root-mean square amplitude was computed to quantify the degree of muscular activation between conditions. The rest period (30 s) collected at the beginning of CKC recordings was considered as a baseline representative of a relaxed condition (i.e. without volitional muscular activation) and it was compared to the corresponding *active* and *passive* conditions to evaluate the presence and degree of the muscular activity of soleus and tibialis anterior. To this end, we conducted a Wilcoxon signed rank test (non-parametric statistical test) to search for statistically

significant differences between the muscular activity during rest, *active* and *passive* conditions. We considered merged trials for the abovementioned comparison.

Statistical significance of CKC

The hypothesis of linear independence of Fourier coefficients at each frequency between epochs was used to assess the statistical significance of individual coherence levels (21, 48). To correct for multiple comparisons, the significance α-level was set to 0.05/Nc, with Nc number of EEG electrodes, i.e., 30. Because of the non-normal distribution of the data, a Wilcoxon signed rank test (non-parametric test) was used to assess differences between the two trials, separately per each condition to investigate the possibility of pooling trials together to further inspect the effect of muscle activation on CKC.

Effect of volitional muscle activation on CKC

As a result of the non-normal distribution of the data, a non-parametric test (Wilcoxon signed rank test) was used to examine whether CKC strength differed between the *active* and *passive* conditions.

Correlation analysis

To evaluate the associations between CKC and proprioceptive-perception ability, the correlation of CKC strength to the proprioceptive-perception threshold was computed using Spearman rank correlation coefficient.

RESULTS

Figure 2 shows raw EEG, EMG and kinematic signals during rest, active and passive conditions. The overall signal quality was good, without any notable artifact rising from the ankle-movement actuator or the external environment. For both conditions we considered the same, fixed number of independent components (i.e. 30) explaining the 99.28 ± 0.43% of the variation for *active* condition and the 99.46 ± 0.33% for *passive* condition. On average, 3 ± 2 independent components were rejected from EEG signals, while the average number of discarded epochs was 3 ± 3 across conditions and participants. Within the CKC analysis, the number of epochs was fixed at the minimum number of epochs across the four trials and participants, i.e., 468 epochs per trial.

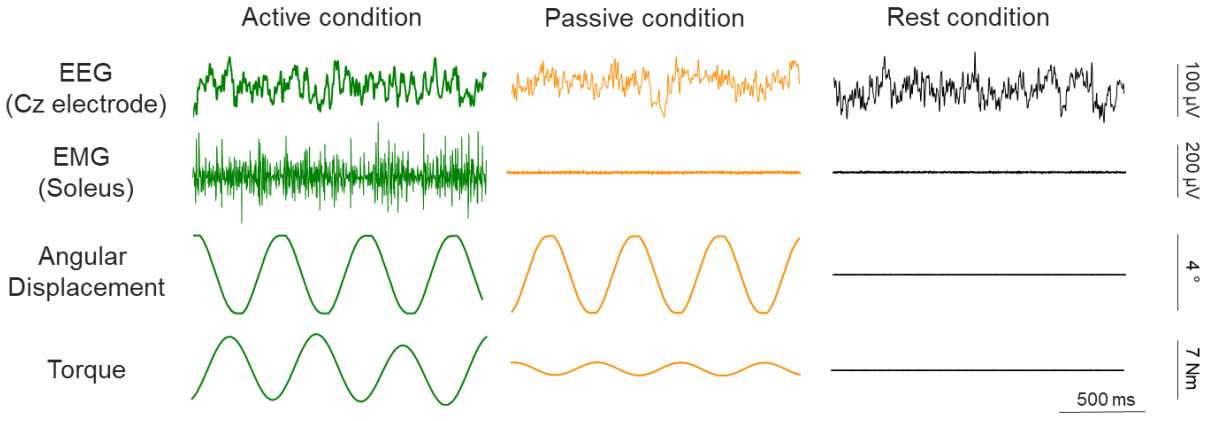

Figure 2 – Example of preprocessed signals form a representative subject during 2 s from active, passive and rest conditions. From top to bottom: EEG from Cz electrode, EMG from soleus muscle, angular displacement and torque applied on the pedal are represented.

EMG activity during proprioceptive stimulations

Figure 3 shows the muscular activation levels in terms of EMG root-mean-square values of *active*, *passive* and rest conditions (merged trials). As expected, activation levels were significantly higher during the active condition than both rest and passive conditions ($P < 0.01$), both for soleus and tibialis anterior muscles without showing any statistically significant differences between *passive* and rest conditions. Although the task mainly required the activity of plantarflexor muscles (i.e. soleus) a slight co-contraction of the tibialis anterior muscle was also noticed.

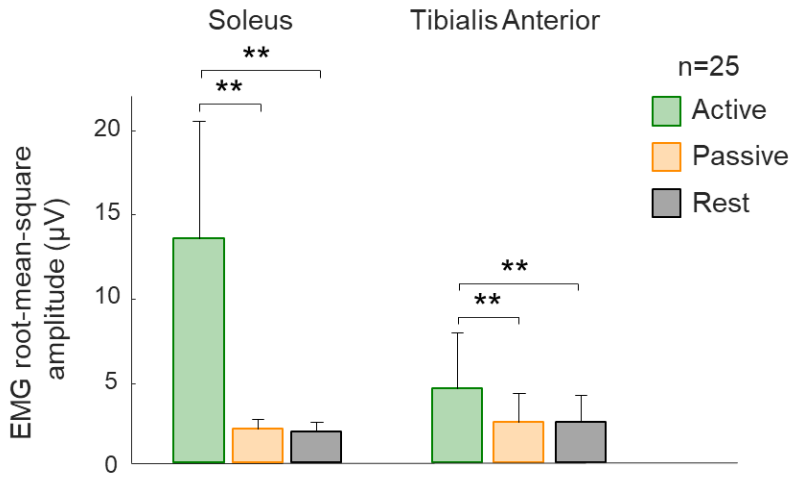

*Figure 3 – Bar diagrams showing the EMG root-mean-square amplitudes (μV) of soleus and tibialis anterior muscles during active, passive and rest conditions averaged across participants. Error bars indicate the standard deviation of the muscular activation levels across participants. Statistical analysis by Wilcoxon signed-rank test, (** P <0.01).*

Corticokinematic coherence

Figure 4 shows the CKC results. At the group level, CKC was stronger during the *active* than *passive* condition ($P < 0.01$). Figure 4 B shows the individual CKC strengths at 2-Hz peak for the Cz electrode for both conditions. Striking increase in CKC was observed in 22 out of 25 participants from *passive* to *active* condition, while only 3 out of 25 participants showed an opposite tendency.

At the individual level, CKC was above the significance level in 21 out of 25 participants at the 2-Hz-movement frequency for the *active* condition and in 11 out of 25 participants for the *passive* one. For all the participants, when above the statistical significance level, CKC was peaking at the level of Cz electrode (i.e. above the midline central scalp region as expected for ankle-joint stimulation) in both conditions. Figure 4 A shows the coherence spectra for the *active* and *passive* conditions for the Cz electrode. The spectra show that the CKC strength was clearly stronger for the *active* than the *passive* condition at 2-Hz peak in the group level (*active* condition: 0.13 ± 0.14, *passive* condition: 0.03 ± 0.04), and peaked at the expected Cz electrode over the foot area of the SM1 cortex in both conditions. Although with weaker CKC values, results at the first harmonic (i.e. at 4 Hz) of the movement frequency confirmed what we found at the 2-Hz movement frequency in terms of spatial distribution and CKC strength trend between conditions (active: 0.04 ± 0.17, passive: 0.02 ± 0.05). Nevertheless, we found only 8/25 (active condition) and 4/25 (passive condition) participants with CKC above the significance level at the first harmonic.

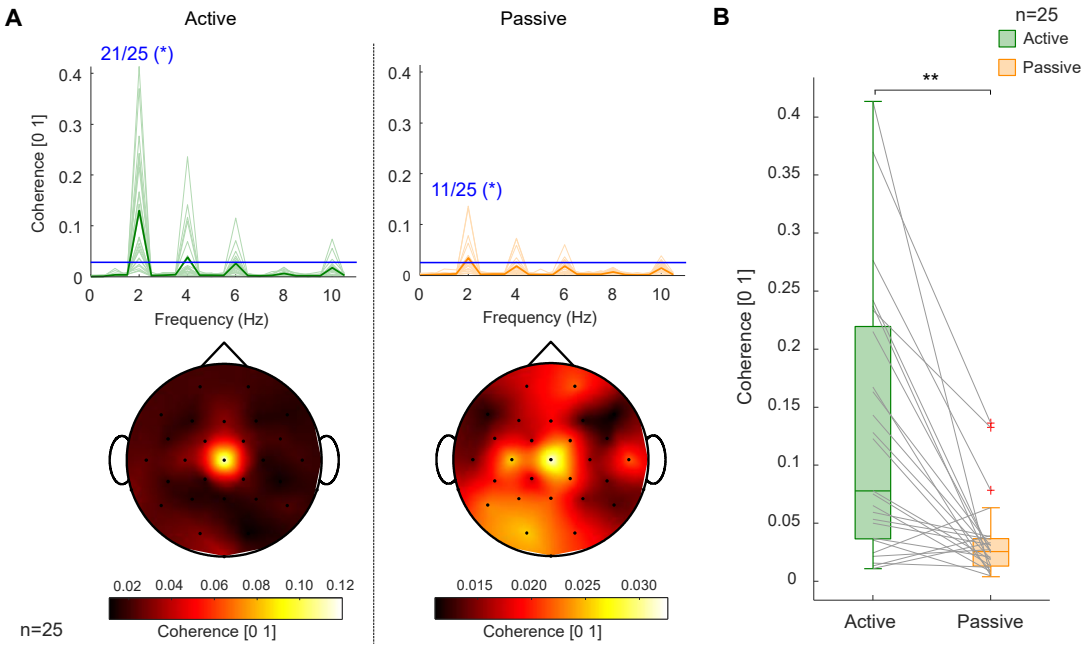

*Figure 4 – Corticokinematic coherence results (n=25). A) CKC spectra of Cz electrode (top panel) and topographic representation of CKC strength at the movement frequency averaged across subjects (bottom panel) for active and passive conditions. The light colored lines indicate the individual spectra, whereas the marked lines indicate the grand-average spectra. Horizontal blue line indicates the statistical significance level. Color bar scales of spatial topographies are different for the two conditions to highlight the spatial distribution of CKC strength over the scalp for both conditions. B) Boxplot representations of Cz-electrode-CKC strengths at the movement frequency for both conditions. Statistical analysis by Wilcoxon signed-rank test, *P<0.05, **P<0.01.*

Correlation between CKC strength and proprioceptive-perception ability

Figure 5 shows the result of the proprioceptive perception ability test for a representative participant (threshold at 0.8 °/s). The average proprioceptive threshold was 0.79 ± 0.19 °/s across the participants.

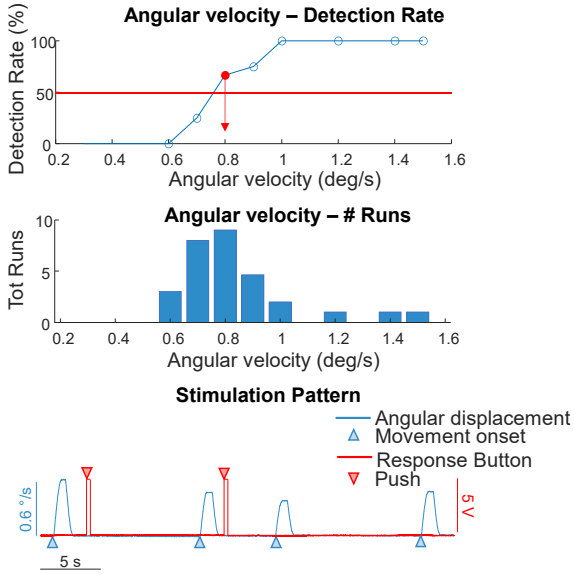

Figure 5 – Evaluation of proprioceptive ability test performances of a representative subject. From top to bottom, representations of: angular velocity-detection rate, angular velocity-number of runs and evaluation of response time.

However, no statistically significant correlation was found between CKC strength and proprioceptive threshold (*active* condition: r = –0.07, P = 0.75; *passive* condition: r = –0.03, P = 0.87; Figure 6).

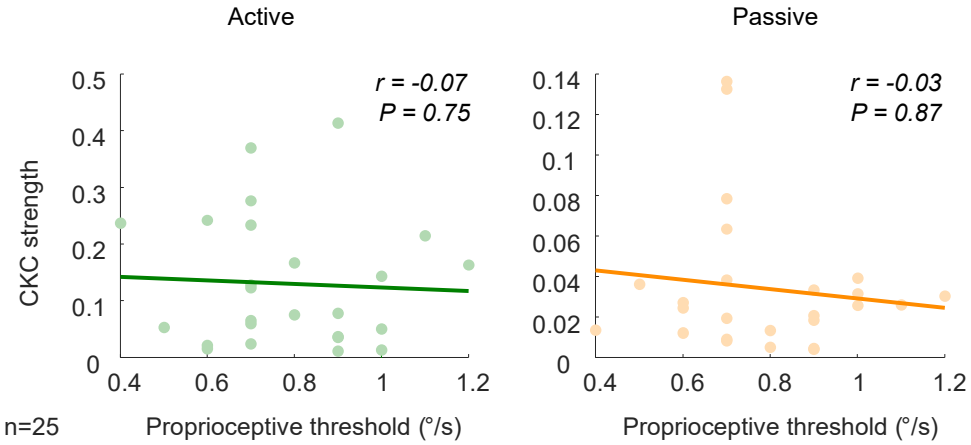

Figure 6 – Correlation between CKC strength at the movement frequency and proprioceptive threshold for active and passive conditions. Pearson correlation coefficients are superimposed, (n=25 participants).

DISCUSSION

Corticokinematic coherence was peaking at movement frequency and at the multiple harmonic frequencies as typically observed in EEG- or MEG-based studies (28, 30). However, as shown by Piitulainen et al., (2020) (34), CKC strength is slightly weaker in EEG than in MEG, also in harmonic frequencies. Therefore, because of the low number of participants with CKC above the significance level, we then performed the analysis focusing on the fundamental 2-Hz movement frequency only. The proprioceptive stimulation of the ankle joint evoked significant CKC in the EEG electrode above the foot region of the SM1 cortex. However, the CKC strength was weaker in the *passive* than *active* stimulation condition, supporting our hypothesis that volitional activation of the stimulated muscles would intensify the cortical proprioceptive processing because of (1) the neuronal and mechanical sensitization of the ankle joint proprioceptors and/or (2) the modulations of the neuronal proprioceptive processing in the spinal and cortical levels due to active motor control processes. This is a significant finding as it may extend the use of CKC method to further examine the cortical neuronal mechanisms related to interplay or closed loop between motor efference and proprioceptive afference during active tasks, and the related adaptations to exercise, rehabilitation and disease.

Effect of muscle activation on CKC

In line with our hypothesis, CKC was stronger during *active* than *passive* condition. From proprioceptors point of view, the main difference between these conditions is the functional state of the muscle spindles and mechanical condition of the ankle joint. The sensitivity of the muscle spindle to muscle-tendon length change is increased during active contractions (36, 37). This is because, the motor efference activating the muscles is accompanied with simultaneous activation of the intrafusal fibers within the muscle spindle by gamma motoneurons improving the detection of muscle length change (50). It is also noteworthy that the muscle spindle is the predominant proprioceptor providing the proprioceptive afference to the CNS occurring at the mid-region of the range of motion, as was the case for both *active* and *passive* ankle rotations in the present study.

The mechanical state of the ankle-joint also differed between the conditions. During the *active* condition, the constant 5-Nm torque increased the muscle-tendon unit tension and likely reduced the muscle-tendon unit slack, which may increase not only the muscle spindle sensitivity, but also the firing rate of Golgi tendon organs that are responsible for detecting the change in force produced by the muscle or directed to the muscle-tendon unit (6). Therefore, we suggest that the combination of the increased firing rate of the abovementioned proprioceptors results in the intensification of the somatosensory afference to the SM1 cortex. This would in turn intensify the cortical processing of the proprioceptive afference and thus resulting in stronger CKC during *active* than *passive* condition. In addition to the proprioceptors, also the cutaneous tactile receptors may contribute to the enhancement of CKC during the active versus passive condition. The plantar pressure under the sole of the foot is stronger during the active condition as seen in the torque signal in Figure 2. This might allow better activation of deep mechanoreceptors of the skin. To alleviate this difference, we used straps around the mid-foot to enhance the plantar pressure during the passive condition, and thus most of the plantar cutaneous receptors were likely activated in both conditions. The evoked movement inevitably also activates the tactile receptors in the skin around ankle joint as the skin is being rhythmically stretched. However, the kinematics of the evoked movements were identical between active and passive conditions, thus a similar tactile afference is expected to occur. Finally, we do not consider this tactile activation strictly as a confounding factor, but as one of the plausible mechanisms for the stronger CKC during the active condition. The brain utilizes the tactile and proprioceptive afference in integrated manner, and thus it is difficult or even unnecessary to separate them when examining naturalistic stimuli.

The brain can also modify its own somatosensory feedback both at spinal and cortical levels (51). Thus, the cortex may actively control its proprioceptive afference and spinal level sensorimotor processing. This mechanism is especially evident during the active maintenance of the isometric contraction in the *active* condition. Therefore, it is likely that the spinal, medullary and thalamic circuits influencing the afferent proprioceptive pathways to the SM1 cortex are modulated in a way that intensifies the associated cortical processing with respect to the *passive* condition. Such modulation can be also influenced by cortico-cortical connections. Thus, different cortical regions related to motor control and somatosensation can contribute to influence the SM1 cortex processing of proprioceptive afference during the *active* motor task. This interpretation is in line with earlier observation on rodents. It has been shown that focal enhancement of rat motor cortex activity facilitated sensory-evoked responses of topographically aligned neurons in the primary somatosensory cortex (52).

The state of the SM1 cortex may also affect the CKC strength. It is well established that the SM1 cortex is activated just prior (i.e. motor preparation) and during (i.e. due to both volitional motor output and somatosensory input) volitional muscle contraction. The state of SM1 cortex is altered also during the passive rotations of the ankle due to the consequent strong proprioceptive afference to the SM1 cortex. Nevertheless, the volitional motor processes are not effective in similar manner in *active* versus *passive* condition. As an example, Piitulainen et al., (2013) (53) investigated CKC during active (i.e. self-performed) versus passive finger movements and they did not observe differences in CKC strength, spatial location or coherence directionality between the conditions. Although, this result might seem in contrast to ours (i.e. strengthened CKC during active versus passive condition), the active task fundamentally differed between these studies, and thus the results are not directly comparable. Piitulainen et al., (2013) (53) used self-paced (i.e. active) dynamic finger movements. On the contrary, the current task was to maintain steady plantarflexion torque despite externally evoked perturbations (i.e. rotations) to the ankle joint.

Thus, our active task did not include active movement, but active stabilisation of the ankle joint. In addition, different limbs were investigated (hand versus foot), thus we could not make any inferences between studies. Additionally, also the sensorimotor processes are partly different between *active* and *passive* condition. Indeed, CKC strength has been shown to be increased when attention is directed to the proprioceptive stimulation when compared to situation in which the attention was directed away from the stimulation to a visual task in passive conditions (29). In our *active* task, the attention was directed to the proprioceptive-motor task to stabilize the quasi-steady plantarflexion. The task was rather challenging since the ankle was being passively rotated simultaneously. Instead, during the *passive* condition, although attention was not expressively directed to the proprioceptive stimulation, participants followed the stimulations without being distracted by another visual or motor task. Consequently, these attentional differences may partly explain the enhanced CKC strength during *active* condition, but the attentional effects are expected only to minimally affect the dramatic difference in CKC strength between the conditions in the current study. Previous evidence demonstrated only a minor reduction in CKC strength (~9%) when attention was directed to the proprioceptive stimulation or away from it to a visual task (29). Indeed, given that there might have been more attention to the foot or to the stimulus during the *active* condition, this should have led to reduction in CKC, but we observed the opposite.

It is worth mentioning that less than 50% of our participants showed significant CKC at the movement frequency during the *passive* condition. This was somewhat surprising as strong CKC has been observed for ankle joint rotations in MEG (32). However, to the best of our knowledge, there are no EEG-based CKC studies involving passive stimulation for the lower limbs. Most of the CKC studies have focused on passive or self-performed upper limb movements in MEG (18, 21–23). For the passive hand stimulation, CKC strength has shown to be weaker for EEG than MEG (34). Furthermore, the use of spatial filters (i.e. bipolar, Laplacian filters) and 58-electrode EEG cap enhanced CKC strength when compared to common reference filter (34). However, we recently showed that the improvement associated with spatial filtering when using a 30-electrode EEG cap is not systematically observed with less dense EEG electrode caps (35). Therefore, we did not use of a spatial filters (bipolar or Laplacian) in the current study. Nevertheless, the use of a more dense EEG cap could be suggested for future CKC studies using passive proprioceptive stimulation of the ankle joint and EEG recordings for the abovementioned reasons. The more spatially selective EEG derivations could enhance detection of CKC above the significance level also in the lower limbs.

Furthermore, the weak CKC may be specific to the lower limbs in comparison to the upper limbs, that are more widely investigated using CKC (19, 21, 34) with respect to the few MEG lower limbs studies (16, 32). Firstly, the cortical representation of the hand region in the SM1 cortex is more optimally located and oriented for EEG/MEG compared to the foot region that is located deeper and centrally in the posterior paracentral lobule, that is a U-shaped convolution that loops below the medial part of the central sulcus thus resulting in a deep localization of the source (54). The hand area is also wider with respect to the lower limb one. Consequently, non-invasive EEG recordings of cortical signals from the scalp surface will result in weaker signal-to-noise ratio negatively influencing CKC strength.

Correlation between CKC and proprioceptive-perception ability

The proprioceptive-perception ability of the tested population was in line with the result of our previous studies on young healthy adults (39). We did not detect a significant correlation between behavioral and cortical (i.e. CKC strength) proprioception. Thus, our hypothesis that lower

proprioceptive-perception threshold (i.e. better behavioral performance) would be associated with weaker CKC was not supported. Nevertheless, it is worth mentioning that our sample consisted of a rather homogeneous population of highly performing healthy young adults without proprioceptive deficits. Therefore, the variation in behavioral proprioceptive performance was small. This potential association should be further examined in samples with more variable proprioceptive performance, such as cerebral palsy, developmental coordination disorder or older adults (32, 38).

Perspectives and Significance

The present study is the first investigating the effect of volitional muscle activation on EEG-based CKC assessment of cortical proprioception of the ankle joint. We demonstrated that CKC was stronger when the muscles were active during proprioceptive ankle-joint stimulation when compared to *passive* stimulation condition. The intensified cortical proprioceptive processing may be related to neuronal and mechanical differences between *active* and *passive* conditions at muscle-tendon unit, receptor, spinal, medullar, thalamic and cortical levels. The proposed methods and technologies could be further adopted in future research to deepen the understanding and adaptation of the cortical proprioceptive processing during active motor tasks. As such these measures will become potential tools to evaluate also the effects of ageing or neurological diseases such as stroke, Parkinson's or developmental diseases to cortical proprioception.

DATA AVAILABILITY

The data are not publicly available due to privacy or ethical restrictions. However, data are available upon request from the corresponding author.

ACKNOWLEDGMENTS

We thank the chief technician Sakari Vekki from University of Jyväskylä for his technical support in building the experimental design.

GRANTS

This study was supported by the Academy of Finland (grants #296240, #327288 and #326988 to H.P.), and "Brain changes across the life-span" profiling funding to University of Jyväskylä (grant #311877). A.G. is supported by a three-year PhD fellowship from Politecnico di Torino, Turin, Italy.

DISCLOSURES

The authors declare that the study was conducted in the absence of any commercial or financial relationships that could be construed as a potential conflict of interest.

AUTHOR CONTRIBUTIONS

H.P. conceived and designed the research; A.G. performed experiments, A.G., G.L.C., A.B. and H.P. analyzed data; A.G. prepared figures; A.G. and H.P. interpreted results of experiments, A.G. and H.P. drafted the manuscript, A.G., G.L.C., A.B. and H.P. edited and revised the manuscript; A.G., G.L.C., A.B. and H.P. approved the final version of manuscript.

REFERENCES

1. **Moon KM**, **Kim J**, **Seong Y**, **Suh BC**, **Kang KJ**, **Choe HK**, **Kim K**. Proprioception, the regulator of motor function. *BMB Rep* 54: 393–402, 2021. doi: 10.5483/BMBRep.2021.54.8.052.
2. **Grace Gaerlan M**, **Alpert PT**, **Cross C**, **Louis M**, **Kowalski S**. Postural balance in young adults: The role of visual, vestibular and somatosensory systems. *J Am Acad Nurse Pract* 24: 375–381, 2012. doi: 10.1111/j.1745-7599.2012.00699.x.
3. **MEANS JH**. The integrative action of the endocrine system. *Ann. Intern. Med.* 34: 1311–1323, 1951.
4. **Proske U**, **Gandevia SC**. The proprioceptive senses: Their roles in signaling body shape, body position and movement, and muscle force. *Physiol Rev* 92: 1651–1697, 2012. doi: 10.1152/physrev.00048.2011.
5. **Van Beers RJ**, **Baraduc P**, **Wolpert DM**. Role of uncertainty in sensorimotor control. *Philos Trans R Soc B Biol Sci* 357: 1137–1145, 2002. doi: 10.1098/rstb.2002.1101.
6. **Purves D**, **Augustine JG**, **Fitzpatrick D**, **Hall CW**, **LaMantia A-S**, **Mooney DR**, **Platt LM**, **White EL**. *Neuroscience*. 7th ed. Oxford University Press Inc., 2018.
7. **Tuthill JC**, **Azim E**. Proprioception. *Curr Biol* 28: R194–R203, 2018. doi: 10.1016/j.cub.2018.01.064.
8. **Khurana S**. Proprioception: An Evidence Based Narrative Review. *Res Investig Sport Med* 1: 13–17, 2017. doi: 10.31031/rism.2017.01.000506.
9. **Gordon JC**, **Holt NC**, **Biewener A**, **Daley MA**. Tuning of feedforward control enables stable muscle force-length dynamics after loss of autogenic proprioceptive feedback. *Elife* 9: 1–23, 2020. doi: 10.7554/eLife.53908.
10. **Arnin J**, **Yamsa-ard T**, **Triponyuwasin P**, **Wongsawat Y**. Development of practical functional electrical stimulation cycling systems based on an electromyography study of the Cybathlon 2016. *Eur J Transl Myol* 27: 295–301, 2017. doi: 10.4081/ejtm.2017.7111.
11. **Wong JD**, **Kistemaker DA**, **Chin A**, **Gribble PL**. Can proprioceptive training improve motor learning? *J Neurophysiol* 108: 3313–3321, 2012. doi: 10.1152/jn.00122.2012.
12. **Konczak J**, **Corcos DM**, **Horak F**, **Poizner H**, **Shapiro M**, **Tuite P**, **Volkmann J**, **Maschke M**. Proprioception and Motor Control in Parkinson's Disease. *J Mot Behav* 41: 543–552, 2009. doi: 10.3200/35-09-002.
13. **Lephart SM**, **Pincivero DM**, **Giraldo JL**, **Fu FH**. The role of proprioception in the management and rehabilitation of athletic injuries. *Am J Sports Med* 25: 130–137, 1997. doi: 10.1177/036354659702500126.
14. **Toledo DR**, **Manzano GM**, **Barela JA**, **Kohn AF**. Cortical correlates of response time slowing in older adults: ERP and ERD/ERS analyses during passive ankle movement. *Clin Neurophysiol* 127: 655–663, 2016. doi: 10.1016/j.clinph.2015.05.003.
15. **Brey H**. Performance Evaluation for a Class of Asymetrically Ablated Duroid Radomes. *Sci Sin* 2015: 117–127, 1980.
16. **Mujunen T**, **Seipäjärvi S**, **Nurminen M**, **Parviainen T**, **Piitulainen H**. Reproducibility of evoked and induced MEG responses to proprioceptive stimulation of the ankle joint. *Neuroimage: Reports* 2: 100110, 2022. doi: 10.1016/j.ynirp.2022.100110.
17. **Seiss E**, **Hesse CW**, **Drane S**, **Oostenveld R**, **Wing AM**, **Praamstra P**. Proprioception-related evoked potentials: Origin and sensitivity to movement parameters. *Neuroimage* 17: 461–468, 2002. doi: 10.1006/nimg.2002.1211.
18. **Nurmi T**, **Hakonen M**, **Bourguignon M**, **Piitulainen H**. Proprioceptive response strength in the primary sensorimotor cortex is invariant to the range of finger movement. *Neuroimage* 269: 119937, 2023. doi: 10.1016/j.neuroimage.2023.119937.
19. **Smeds E**, **Vanhatalo S**, **Piitulainen H**, **Bourguignon M**, **Jousmäki V**, **Hari R**. Corticokinematic coherence as a new marker for somatosensory afference in newborns

[Online]. *Clin Neurophysiol* 128: 647–655, 2017. http://dx.doi.org/10.1016/j.clinph.2017.01.006.
20. **Jerbi K**, **Lachaux JP**, **N'Diaye K**, **Pantazis D**, **Leahy RM**, **Garnero L**, **Baillet S**. Coherent neural representation of hand speed in humans revealed by MEG imaging. *Proc Natl Acad Sci U S A* 104: 7676–7681, 2007. doi: 10.1073/pnas.0609632104.
21. **Bourguignon M**, **De Tiège X**, **de Beeck MO**, **Pirotte B**, **Van Bogaert P**, **Goldman S**, **Hari R**, **Jousmäki V**. Functional motor-cortex mapping using corticokinematic coherence. *Neuroimage* 55: 1475–1479, 2011. doi: 10.1016/j.neuroimage.2011.01.031.
22. **Bourguignon M**, **Piitulainen H**, **De Tiège X**, **Jousmäki V**, **Hari R**. Corticokinematic coherence mainly reflects movement-induced proprioceptive feedback. *Neuroimage* 106: 382–390, 2015. doi: 10.1016/j.neuroimage.2014.11.026.
23. **Piitulainen H**, **Bourguignon M**, **De Tiège X**, **Hari R**, **Jousmäki V**. Corticokinematic coherence during active and passive finger movements. *Neuroscience* 238: 361–370, 2013. doi: 10.1016/j.neuroscience.2013.02.002.
24. **Bourguignon M**, **Jousmäki V**, **Dalal SS**, **Jerbi K**, **De Tiège X**. Coupling between human brain activity and body movements: Insights from non-invasive electromagnetic recordings. *Neuroimage* 203, 2019. doi: 10.1016/j.neuroimage.2019.116177.
25. **Bourguignon M**, **Jousmäki V**, **Op de Beeck M**, **Van Bogaert P**, **Goldman S**, **De Tiège X**. Neuronal network coherent with hand kinematics during fast repetitive hand movements. *Neuroimage* 59: 1684–1691, 2012. doi: 10.1016/j.neuroimage.2011.09.022.
26. **Piitulainen H**, **Bourguignon M**, **De Tiège X**, **Hari R**, **Jousmäki V**. Coherence between magnetoencephalography and hand-action-related acceleration, force, pressure, and electromyogram [Online]. *Neuroimage* 72: 83–90, 2013. http://dx.doi.org/10.1016/j.neuroimage.2013.01.029.
27. **Piitulainen H**, **Bourguignon M**, **Hari R**, **Jousmäki V**. MEG-compatible pneumatic stimulator to elicit passive finger and toe movements [Online]. *Neuroimage* 112: 310–317, 2015. http://dx.doi.org/10.1016/j.neuroimage.2015.03.006.
28. **Piitulainen H**, **Illman M**, **Laaksonen K**, **Jousmäki V**, **Forss N**. Reproducibility of corticokinematic coherence. *Neuroimage* 179: 596–603, 2018. doi: 10.1016/j.neuroimage.2018.06.078.
29. **Piitulainen H**, **Nurmi T**, **Hakonen M**. Attention directed to proprioceptive stimulation alters its cortical processing in the primary sensorimotor cortex. *Eur J Neurosci* 54: 4269–4282, 2021. doi: 10.1111/ejn.15251.
30. **Mujunen T**, **Nurmi T**, **Piitulainen H**. Corticokinematic coherence is stronger to regular than irregular proprioceptive stimulation of the hand. *J Neurophysiol* 126: 550–560, 2021. doi: 10.1152/jn.00095.2021.
31. **Hakonen M**, **Nurmi T**, **Vallinoja J**, **Jaatela J**, **Piitulainen H**. More comprehensive proprioceptive stimulation of the hand amplifies its cortical processing. *J Neurophysiol* 128: 568–581, 2022. doi: 10.1152/jn.00485.2021.
32. **Piitulainen H**, **Seipäjärvi S**, **Avela J**, **Parviainen T**, **Walker S**. Cortical proprioceptive processing is altered by aging. *Front Aging Neurosci* 10: 1–13, 2018. doi: 10.3389/fnagi.2018.00147.
33. **Démas J**, **Bourguignon M**, **De Tiège X**, **Wens V**, **Coquelet N**, **Rovai A**, **Bouvier S**, **Bailly R**, **Brochard S**, **Dinomais M**, **Van Bogaert P**. Assessing spino-cortical proprioceptive processing in childhood unilateral cerebral palsy with corticokinematic coherence. *Neurophysiol Clin* 52: 33–43, 2022. doi: 10.1016/j.neucli.2021.12.003.
34. **Piitulainen H**, **Illman M**, **Jousmäki V**, **Bourguignon M**. Feasibility and reproducibility of electroencephalography-based corticokinematic coherence. *J Neurophysiol* 124: 1959–1967, 2020. doi: 10.1152/jn.00562.2020.
35. **Giangrande A**, **Cerone GL**, **Gazzoni M**, **Botter A**, **Piitulainen H**. Quantification of cortical proprioceptive processing through a wireless and miniaturized EEG amplifier.

Proc Annu Int Conf IEEE Eng Med Biol Soc EMBS 2022-July: 4797–4800, 2022. doi: 10.1109/EMBC48229.2022.9871637.

36. **Edin BYBB**, **Vallbo AKEB**. Physiology, Umed University, S-901 87 Umed,. .
37. **Ribot-Ciscar E**, **Tardy-Gervet MF**, **Vedel JP**, **Roll JP**. Post-contraction changes in human muscle spindle resting discharge and stretch sensitivity. *Exp Brain Res* 86: 673–678, 1991. doi: 10.1007/BF00230541.
38. **Piitulainen H**, **Nurmi T**, **Vuontela V**, **Mäenpää H**, **Lano A**, **Carlson S**. Perception of the ankle joint proprioception is impaired in extremely preterm-born adolescents and is associated with weaker fine-motor performance. *Gait Posture* 97: S159–S160, 2022. doi: 10.1016/j.gaitpost.2022.07.105.
39. **Piitulainen H**, **Nurmi T**, **Vuontela V**, **Mäenpää H**, **Lano A**, **Carlson S**. Proprioceptive perception of the ankle joint is impaired in developmental coordination disorder. *Gait Posture* 90: 188–189, 2021. doi: 10.1016/j.gaitpost.2021.09.098.
40. **Isman RE**, **Inman VT**. Anthropometric Studies of the Human Foot and Ankle [Online]. *Foot Ankle* 11: 97–129, 1969. http://www.rehab.research.va.gov/jour/69/6/1/97.pdf.
41. **Cerone GL**, **Giangrande A**, **Ghislieri M**, **Gazzoni M**, **Piitulainen H**, **Botter A**. Design and Validation of a Wireless Body Sensor Network for Integrated EEG and HD-sEMG Acquisitions. *IEEE Trans NEURAL Syst Rehabil Eng* 30: 2022, [date unknown]. doi: 10.1109/TNSRE.2022.3140220.
42. **Cerone GL**, **Botter A**, **Gazzoni M**. A modular, smart, and wearable system for high density sEMG detection. *IEEE Trans Neural Syst Rehabil Eng* 66: 3371–3380, 2019.
43. **Cerone GL**, **Gazzoni M**. A wireless, minaturized multi-channel sEMG acquisition system for use in dynamic tasks. In: *2017 IEEE Biomedical Circuits and Systems Conference, BioCAS 2017 - Proceedings*. 2018.
44. **Stegeman D**, **Hermens H**. Standards for surface electromyography: The European project Surface EMG for non-invasive assessment of muscles (SENIAM) [Online]. http://www.seniam.org/%5Cnhttp://www.med.uni-jena.de/motorik/pdf/stegeman.pdf.
45. **Merletti R**, **Cerone GL**. Tutorial. Surface EMG detection, conditioning and pre-processing: Best practices. *J Electromyogr Kinesiol* 54: 102440, 2020. doi: https://doi.org/10.1016/j.jelekin.2020.102440.
46. **Oostenveld R**, **Fries P**, **Maris E**, **Schoffelen J**. FieldTrip : Open Source Software for Advanced Analysis of MEG , EEG , and Invasive Electrophysiological Data. 2011, 2011. doi: 10.1155/2011/156869.
47. **McFarland DJ**, **McCane LM**, **David S V.**, **Wolpaw JR**. Spatial filter selection for EEG-based communication. *Electroencephalogr Clin Neurophysiol* 103: 386–394, 1997. doi: 10.1016/S0013-4694(97)00022-2.
48. **Halliday DM**, **Rosenberg JR**, **Amjad AM**, **Breeze P**, **Conways BA**, **Farmer SF**. A framework for the analysis of mixed time series/point process data - theory ad application to the study of physiological tremor, single motor unit discharges and electromyograms. 237–278, 1995.
49. **Bortel R**, **Sovka P**. Approximation of statistical distribution of magnitude squared coherence estimated with segment overlapping. *Signal Processing* 87: 1100–1117, 2007. doi: 10.1016/j.sigpro.2006.10.003.
50. **Khan MN**, **Cherukuri P**, **Negro F**, **Rajput A**, **Fabrowski P**, **Bansal V**, **Lancelin C**, **Lee TI**, **Bian Y**, **Mayer WP**, **Akay T**, **Müller D**, **Bonn S**, **Farina D**, **Marquardt T**. ERR2 and ERR3 promote the development of gamma motor neuron functional properties required for proprioceptive movement control. 2022.
51. **McIlroy WE**, **Bishop DC**, **Staines WR**, **Nelson AJ**, **Maki BE**, **Brooke JD**. Modulation of afferent inflow during the control of balancing tasks using the lower limbs. *Brain Res* 961: 73–80, 2003. doi: 10.1016/S0006-8993(02)03845-3.
52. **SooHyun L**, **George EC**, **Daniel JS**. Motor modulation of afferent somatosensory

circuits. *Nat Neurosci* 11: 1430–1438, 2008. doi: 10.1038/nn.2227.Motor.
53. **Piitulainen H**, **Bourguignon M**, **De Tiège X**, **Hari R**, **Jousmäki V**. Corticokinematic coherence during active and passive finger movements. *Neuroscience* 238: 361–370, 2013. doi: 10.1016/J.NEUROSCIENCE.2013.02.002.
54. **Rao SM**, **Binder JR**, **Hammeke TA**, **Bandettini PA**, **Bobholz JA**, **Frost JA**, **Myklebust BM**, **Jacobson RD**, **Hyde JS**. Somatotopic mapping of the human primary motor cortex with functional magnetic resonance imaging. *Neurology* 45: 919–924, 1995. doi: 10.1212/WNL.45.5.919.